Research Article | Vol. 27, No. 17 / 19 August 2019 / Optics Express 24434
Optics EXPRESS

Measured radiation effects on InGaAsP/InP ring resonators for space applications

GIUSEPPE BRUNETTI,[1] IAIN MCKENZIE,[2] FRANCESCO DELL'OLIO,[1] MARIO N. ARMENISE,[1] AND CATERINA CIMINELLI[1,*]

[1] *Optoelectronics Laboratory, Politecnico di Bari, 70125 Bari, Italy*
[2] *European Space Agency (ESA), ESTEC, Keplerlaan 1, PO Box 299, NL-2200 AG Noordwijk, The Netherlands*
[*] *caterina.ciminelli@poliba.it*

Abstract: Photonic ring resonators can be considered building blocks of new concept satellite payloads for implementing several functions, such as filtering and sensing. In particular, the use of a high Q-factor ring resonator as sensing element into a *Resonant Micro Optic Gyroscope* (RMOG), provides a remarkable improvement of the performance with respect to the competitive technologies. To qualify a ring resonator for Space applications, the radiation effects on it in the Space must be carefully evaluated. Here, we investigate the effects of gamma radiation on a high Q InGaAsP/InP ring resonator, for the first time, to our knowledge. The ring resonator under study has a footprint of about 530 mm^2 and it is based on a InGaAsP/InP rib waveguide, with a width of 2 µm and a thickness of 0.3 µm, formed on a 0.7 µm thick slab layer on an InP substrate 625 µm thick. For a total dose of about 320 krad *Co60* gamma irradiation, a mean variation of about 13% and 4% was measured for Q and *extinction ratio* (*ER*), respectively, with respect to the values before irradiation ($Q = 1.36 \times 10^6$, $ER = 6.24$ dB). Furthermore, the resonance peak red-shifts with a linear behaviour was observed increasing the total dose of the absorbed radiation, with a maximum resonance detuning of about 810 pm. These non-significant effects of a quite high gamma radiation dose confirm the potential of high-Q InP-based ring resonators into Space systems or subsystems.

1. Introduction

The radiation environment affects the operation of the spacecraft instruments and it represents a hazard for the success of a Space mission. The radiation harmful effects are strictly related to its intrinsic nature [1,2]. Radiation can be either non-ionizing or ionizing, with low ($< \sim 10$ eV) or high ($> \sim 10$ eV) energy, respectively [3]. In contrast to non-ionizing radiation that can easily be shielded out, the ionizing radiation is much more difficult to neutralize. The most important causes of the ionizing radiations in Space could be associated to: (1) protons and nuclei of Galactic origin, called *Galactic Cosmic Radiation* (CGR), (2) protons and nuclei emitted by Solar flares and Coronal Mass Ejections, also known as *Solar Energetic Particles* (SEPs), (3) trapped protons in the Van Allen Belts [4]. As detected by the satellite-borne space mission in the PAMELA experiment [5] over three years, the measured total final ionizing radiation dose is equal to about 1 krad, resulting by a detected total dose related to the CGRs and SEPs equal to 0.4 krad and 0.5 krad, respectively [6].

According to the radiation nature, the ionizing rays are classified as α, β and γ rays, in terms of penetration capability and related energy. In particular, the gamma rays could undermine even permanently the correct operation of a device, due to their large capability of penetrating into the shield, although their ionising potential is less than other ionizing rays. When a gamma ray passes through matter, the probability for its absorption is proportional to the thickness, to the density and to the absorption cross-section of the material. Three gamma radiation ionizing processes

#361754 https://doi.org/10.1364/OE.27.024434
Journal © 2019 Received 6 Mar 2019; revised 11 Jun 2019; accepted 11 Jun 2019; published 13 Aug 2019

Optics EXPRESS

can be considered: the photoelectric effect, the Compton scattering, and the electron-positron pair production [7,8]. Compton scattering is the principal absorption mechanism for gamma rays in the intermediate energy range from 100 keV to 10 MeV. For energy higher than 5 MeV, the most important absorption mechanism is the electron-positron pair production. By interaction with the electric field of a nucleus, the energy of the incident photon is converted into the mass of an electron-positron pair, and then, their annihilation produces two gamma photons of at least 0.51 MeV energy each [9].

Each aforementioned physical process or the combination of some of them could degrade and/or permanently damage the operation of the on-board electronics in a Space mission. In literature several papers have been proposed on the evaluation of the radiation hardness of electronic devices [4,10,11]. As shown in [11], the degradation of a transistor performance has been observed when exposed to gamma radiation. In particular, the operation of electronic devices is affected by the damaging ionizing effect, resulting in a change of the carrier's concentration and then a change of the device features, as the voltage threshold for a transistor [11].

In the last decades, a strong research effort has been focused on the improvement of the radiation hardness of the on-board instruments, because no replacement is possible once the instruments are in orbit. A photonic approach could help in achieving higher radiation resistance, together with the well-known advantages with respect to the electronics, as small size, robustness, high degree of integration and costs potentially lower [12,13].

The effect of ionizing radiation in Space has been reported in several papers on discrete optics (as LEDs, laser sources) [14–20] and on fiber optics [21–23]. The behaviour of these devices under radiation is characterized by a non-ionizing damage, resulting by the Compton scattering. In addition, optical components, especially optical fibers and fiber-based components, e.g. fiber Bragg gratings, suffer from radiation-induced densification/compaction that causes refractive index changes [22,24]. This effect justifies the change of the optical properties which can lead to an increase of the losses and to a shift of the operating wavelength [25].

According to the rising use of the high quality factor and compact size ring resonators, in the last decades, as fundamental components of integrated photonic circuits, such as the ones for optical filtering, frequency comb generation and sensing [26], the radiation impact on their performance in space applications, is of strong interest [16–19]. Ring resonators are key elements in the *RMOGs*, able to satisfy the demands in terms of compactness and resolution (e.g. gyro sensitivity in the range 0.1–0.01°/s) in moving systems, as guidance, navigation or control systems, both in aircrafts and spacecrafts [27]. The gyroscope performance of ring resonator-based optical gyroscope is strictly related to the Q-factor of the ring, which depends on the intrinsic optical loss due to the absorption as well as the operating wavelength that could be affected by the gamma radiation. In particular, as reported in [18], the radiation involves a Compton scattering and, in turn, the change of the refractive index and of the optical losses. The effect of radiation has been investigated in ring resonators based on silicon [17–19] and silicon nitride [16]. In particular, the effect of radiation on the resonance of a silicon ring resonator, in terms of Q-factor and operation wavelength shift, is negligible. Baets *et al.* [18] have experimentally demonstrated a linear blue shift of the resonance of a ring resonator with $Q \approx 5 \times 10^3$, with a slope of 0.33 pm/krad, observing a decrease of the optical power of about 8 dBm with a total absorbed dose of 300 krad. Recently, the silicon hardness to radiation has been confirmed also for a Si ring resonator with a high Q factor [19]. In particular, for ring resonators with Q-factor ranging from 5×10^3 to 3×10^4, the spectral response does not show a dose-dependent change in the free spectral range, the Q-factor and the peak position. Immunity to radiation has been shown also for silicon nitride-based ring resonators. Kippenberg *et al.* [16] have demonstrated the radiation hardness of Si_3N_4 resonators, showing a shift of the operation wavelength and a variation of the resonance Q-factor, both negligible, after a proton radiation up to about 100 MeV. In particular,

Optics EXPRESS

the increase of losses due to the irradiation causes a degradation of Q factor from to 10^6 to 0.5×10^5, in the worst case.

Here, we report on the experimental results of the radiation test on an InGaAsP/InP ring resonator, used as sensitive element into a *RMOG*. Measured results show a linear blue shift of the resonance, with a negligible degradation of the Q-factor and *ER*. These results confirmed the capability of a ring resonator in InP material to be used as key building block in guidance, attitude and control systems.

2. Optical characterization of the InGaAsP/InP ring resonator

The device under test is an InGaAsP/InP-based ring resonator with radius $R = 13$ mm, evanescently coupled to one straight waveguide, as shown in Fig. 1(a). The waveguide has a rib structure, with a width, w_{wg}, equal to 2 µm and a thickness, $t_{wg,}$ equal to 0.3 µm, formed on a 0.7 µm thick slab layer (see Fig. 1(a)). The quasi-*TE* mode supported by the guiding structure exhibits a confinement factor of about 80%, with propagation loss in the range $0.5 \div 0.8$ dB/cm [28]. The end sections of the bus waveguide are tapered in order to enhance the fiber/waveguide coupling. In particular, the waveguide width has been tapered up to 8 µm (core diameter of a standard single mode fiber) and the taper length is 0.2 mm. To obtain a resonance depth of about 8 dB, the gap g between bus and ring resonator has been fixed to 1.444 µm, ensuring a coupling efficiency of about 52% [29].

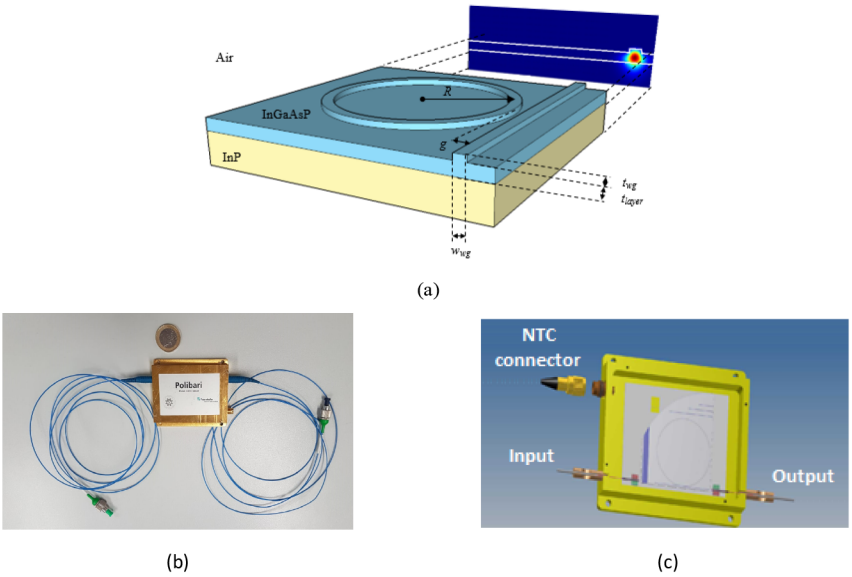

Fig. 1. (a) Schematic of the InGaAsP/InP ring resonator under test, with the map of the electric field of the TE_0 inside the bus waveguide; (b) packaged device under test; (c) schematic of the packaged device.

The ring resonator was fabricated by using a single standard lithography process. First an InGaAsP layer was grown on the top of an InP substrate in a metal-organic vapour-phase-epitaxy (MOVPE) reactor. The waveguide etching was carried out using a thin silicon-nitride layer mask. Finally, the wafer was cleaved and an anti-reflection coating was deposited at the input and output facets of the chip. Further details about the fabrication process can be found in [30].

The device was packaged in a brass case, and lensed single-mode fiber pigtails were connected to the end sections of the bus waveguide, as shown in Fig. 1(b). In order to avoid resonance instability due to temperature changes, a thermo-electric cooler (TEC) was placed beneath

Optics EXPRESS

the resonator chip. Temperature is detected using the transducer AD590 inside the packaging. The packaged ring resonator is sketched in Fig. 1(c), where the two input and output SMF-28 single-mode fibers (1 cm long), and a *NTC* connector, as the TEC output, are shown.

An accurate device characterization has been carried out by measuring the transmission spectrum of the ring resonator under the resonance conditions (see Fig. 2(a)). The laser source used in the set-up is a single-frequency fiber laser (operating wavelength 1.55 µm), with a linewidth < 700 Hz and maximum output power of 30 mW. To detect the resonator spectrum, the laser wavelength has been scanned by using an external piezo-actuator, over a range of 400 MHz across the operating wavelength, driving the laser through a triangle waveform with peak-to-peak amplitude and frequency equal to 20 V and 100 Hz, respectively. Using a polarization controller (*PC*) only one polarization state is excited into the bus waveguide. A typical Lorentzian shaped dip in the transmitted laser power was observed on the oscilloscope screen over the scan time.

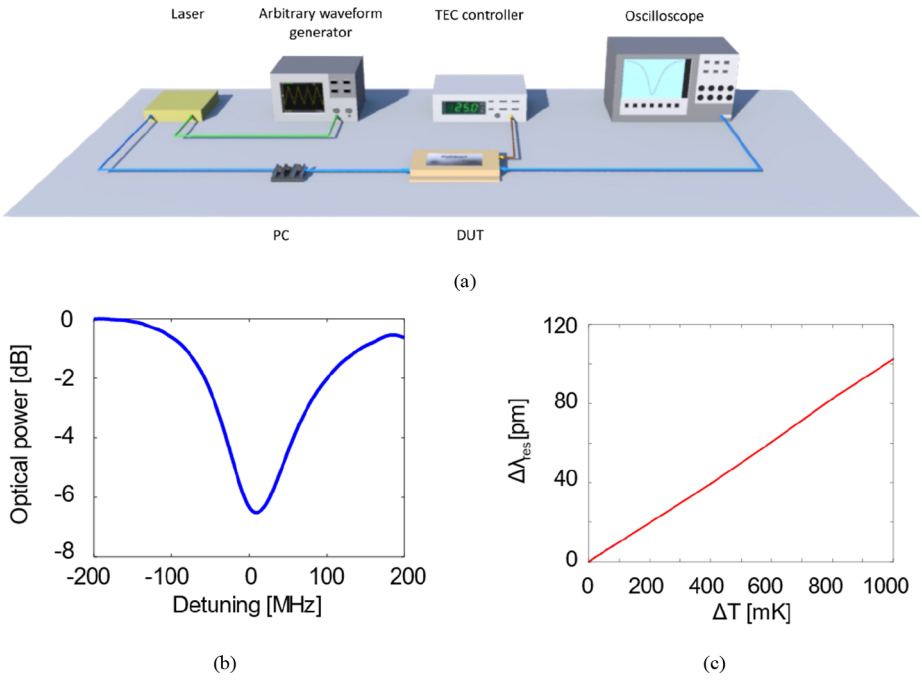

Fig. 2. (a) Overview of the measurement setup; (b) TE mode resonance spectrum; (c) Resonance detuning $\Delta\lambda_{res}$ when changing the chip temperature.

Figure 2(b) shows the measured transmission spectrum of the ring resonator, for a TE polarized input signal, at temperature equal to 25.03 °C. The detection resolution is about 1.6 kHz. For TE mode, the resonance at about 1550 nm shows a $Q = 1.36 \times 10^6$ and $ER = 6.24$ dB. For the TM mode, $Q = 1.35 \times 10^6$ and $ER = 5.75$ dB, have been measured. This performance represents an improvement with respect the one reported in [28], justified by the use of more accurate instruments (i.e. in this work the laser linewidth is about 2 orders of magnitude narrower than the one used in [28]). As shown in Fig. 2(b), the resonance has a typical Fano shape [31], due to the ring resonator backscattering. The achieved experimental results confirmed the use of the device under test as sensitive element in a RMOG configuration. In particular, by using:

$$\delta\Omega = \frac{1}{Qd\sqrt{P_{PD}}}\sqrt{\frac{2hc^3}{\lambda_0\eta\tau_{int}}} \tag{1}$$

Optics EXPRESS

where d is the ring resonator diameter, Q is the ring resonator quality factor, λ_0 is the operating wavelength, τ_{int} is the sensor integration time, P_{PD} is the optical power at the photodiode input, η is the photodetector efficiency, h is the Planck constant and c is the light speed at vacuum [32], a theoretical gyro resolution $\delta\Omega$ equal to about 9 °/h has been estimated (with $P_{PD} = 10$ mW, $\eta = 0.9$, $\tau_{int} = 1$ s). The reverse proportionality between d and $\delta\Omega$ justifies the design of large ring resonator radius ($R = 13$ mm), in order to improve the gyro resolution, in contrast to the compactness.

Moreover, in order to estimate how much the environmental temperature affects the resonance stability, the resonance detuning has been simulated and measured, changing the chip temperature in the range 25.03 °C – 26.03 °C, via the thermo-electric controller. The temperature change involves the effective refractive index change Δn_{eff}, and then, a shift of the resonance $\Delta\lambda_{res}$, according to:

$$\Delta\lambda_{res} = \frac{\Delta n_{eff} \cdot L}{m},\ m = 1, 2, 3, \ldots .. \tag{2}$$

where L is the length of the ring resonator optical path and m is the resonance order [33].

A linear trend of the resonance shit $\Delta\lambda_{res}$ changing the chip temperature with a slope of about 13 MHz/mK has been simulated by using the numerical approach reported in [34], taking into account the refractive index dependence on the temperature (InGaAsP thermo-optic coefficient equal to 2.3×10^{-4} [35]). Performed measurements showed a linear trend with a slope of 12 MHz/mK, as shown in Fig. 2(c), in good agreement with the simulated results.

3. Experimental evaluation of the radiation impact on the InGaAsP/InP ring resonator

In the framework of evaluation of total ionizing dose effects, the estimation of the device hardness under γ radiation represents a conservative approach in Space qualification of an optoelectronics component, being the γ-radiations more dangerous than the other ionizing radiation, as previously described. The experimental activity was carried out following the steps as in [36]. In particular, the protocol for the irradiation test method of the European Cooperation for Space Standardization (*ECSS*) requires three steps: (a) irradiation step, to estimate the impact of the radiation on the device performance; (b) annealing step, to estimate how the device responds to an absence of radiation, shutting down the radiation source; (c) overheating step, to clean the device from any charges present inside, especially in the oxide. The last step requires putting the device under test in an oven at temperatures higher than 100° C. However, this step has not been carried out, wanting to preserve the packaged device for future experiments. This activity has been conducted in the *Co60* facility at *ESTEC* [37], which provides a *Co60* γ source that can radiate photons with energy of the order of 1 MeV. The *Co60* source consists of multiple small rods about 50 mm long placed around the periphery of a 30 mm diameter cylindrical steel container. The source is stored in its own special housing, and when the source is raised to the target position to be irradiated, the γ beam produced by the *Co60* leaves the irradiator unit through a collimator window into the radiation cell. During the experimental characterization, a collimated beam with a dose rate of 99 rad/min has been used to irradiate the packaged ring resonator, mounted with the axis out the chip plane perpendicular to the γ beam at a distance of 52 nm from the irradiator. Only the device under test was mounted in front of the source, while the other instruments (see Fig. 2(a)) were placed in the control room, shielded by the radiation, in order to monitor the device under test. A dosimeter has been used to measure the total absorbed dose. The absorbed dose both in InGaAsP and in brass results from the product of the dosimeter value and the conversion coefficients, as 0.793 for InGaAsP and 0.9 for brass. The dose rate and the working distance have been set taking into account the target total absorbed dose for the ring resonator ($\approx$ 300 krad), the conversion coefficients of InGaAsP and brass, and the thickness of the brass layer placed over the ring resonator ($\approx$ 4.5 mm). The irradiation activity lasted about 68 hours with a total radiation

Optics EXPRESS

dose of about 320 krad absorbed by the ring resonator, followed by an annealing activity for 24 hours.

In order to measure the radiation effects on the resonance frequency, Q and ER, a closed-loop measurement technique has been used. The radiation-induced shift is counteracted by the temperature change imposed by the Peltier effect, driven by the TEC controller. The resonance wavelength is real-time measured through the oscilloscope and the temperature of the TEC controller is regulated in order to set to zero the resonance wavelength variation due to combined and opposed effects of temperature and radiation. Since the resonance is shifted by changing the chip temperature (T_{chip}) and a linear relation λ_{res} vs. T_{chip} has been experimentally observed with a coefficient of about 12 MHz/mK (≈ 0.1 pm/mK), an indirect measure of the radiation-induced shift has been carried out.

The main error source in the measurements is the radiation-induced output current drift of the temperature sensor AD590 in the package. As shown in Fig. 3, the output current of the sensor AD590 decreases by increasing the radiation dose, with a slope S of -0.04 µA/krad (± 7.5%) for T_{chip} = 25 °C and a supply voltage of 5 V. Furthermore, from other experimental measurements, we have observed that the slope S depends also on T_{chip}, with a second-order trend, as shown in Fig. 4. This systematic error has been compensated by a post-processing procedure, based on an accurate mathematical model of the error source. In fact, since the error due to the sensor AD590 on both radiation dose and T_{chip}, has been accurately described by a dedicated experimental activity (see Fig. 4), carried out at the ESA *Co60* facility, the compensation of this error source allows a significant reduction of the measurement uncertainty. This compensation is based on the assumptions that keeping constant the temperature of the sensor AD590, its output current linearly decreases when the dose increases up to 3.25 kGy (Si), as experimentally proved up to the dose of 0.35 kGy (Si). The linear trend that we extrapolated up to 3.25 kGy (Si) is compliant to data available in literature, where a linear trend over 0.35 kGy (Si) has been demonstrated [38].

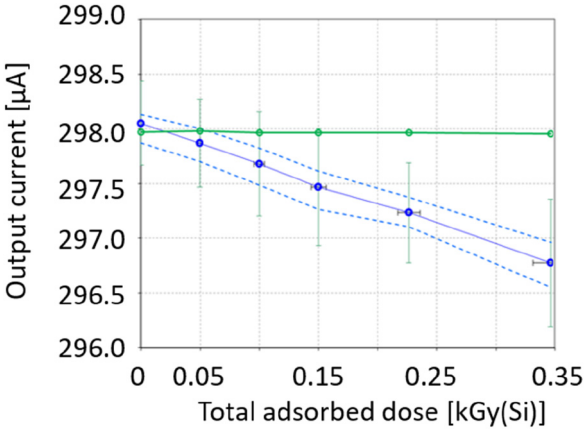

Fig. 3. AD590 output current (blue line) vs total absorbed dose. An output current = 298 µA guarantees a chip temperature equal to 25.0 °C, used as reference (supply voltage = 5 V). The dotted blue lines are referred to the maximum and minimum measured value. The green line is referred to the constant temperature of the chamber, where the measurements are carried out.

Another source error is the accuracy of the TEC controller (± 0.1°C), that causes an error on the resonance wavelength estimation of 0.02%. Furthermore, since the radiation activity required long time, it was necessary to evaluate a possible resonance drift over time due to laser or polarization controller instability. The device resonance without radiation over 16 hours was

Optics EXPRESS

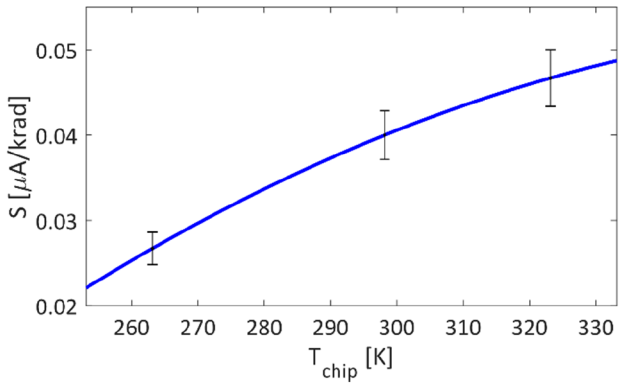

Fig. 4. S [μA/krad] vs T_{chip} [K].

measured, observing a negligible blue-shift of the resonance (< 1 pm), and then, an error on the resonance position of about 4.25 pm at the end of radiation activity.

In order to neglect the radiation impact on the Peltier cell, a closed-loop control has been used to set the chip temperature. The impact of the radiation on the single-mode fibers in the package does not affect the measurements.

The impact of the γ radiation on the TE resonance position, and on the related Q-factor and ER is shown in Figs. 5(a)–5(c), respectively. Over the radiation step, 100 measurements of the resonance were performed. The dominant ionization process in irradiated materials at *Co60* γ radiation energy is the Compton scattering, neglecting any radiation effects on the single-mode fibers connected to the package.

Taking into account all errors on the measurements carried out, an error on the wavelength shift of about 11% has been calculated, mainly caused by the impact of radiation on the sensor AD590 operation. A stochastic distribution of Q-factor and ER has been detected, caused by the dependency of the resonance shape on the polarization and interference effects, which are, in turn, affected by the radiation. Within a small range of radiation energy for values less than 320 krad, Q and ER detected mean variations (ΔQ and ΔER) are equal to about 13% and 4%, respectively (see Figs. 5(b)–5(c)). These variations are caused by a slight change of the optical and coupling losses, although they do not influence the spectrum of a ring resonator, confirmed by the same resonance shape before and after radiation (Fig. 6). The errors on the Q-factor estimation could be considered negligible (±0.001%).

As previously described, the Compton scattering is the main responsible of the resonance shift. In particular, the structural deep point defects, related to the Compton scattering, involve the crystallographic damage, with a consequent change of the refractive index, and then the resonance positions, according to Eq. (2). A fitted linear trend over the radiation time has been derived, with a maximum red-detuning $\Delta\lambda_{res}$ of about 810 pm at the end of irradiation activity. During the annealing step, a blue-shift of the resonance with a second order trend has been observed, with a maximum offset of 60 pm with respect to the resonance position at the end of the irradiation activity. This behaviour is due to relaxation effect on the resonance detected at 320 krad, ending after about 12 hours.

A comparison of results of radiation experiments on devices based on other technology platforms as reported in literature is not easy to carry out, because of different radiation types, energies and dose rates that have been used. In order to rate the InGaAsP/InP-based ring resonator performance, the most appropriate comparison is with radiation experiments on silicon ring resonators, invested by *Co60* γ radiation with a dose rate of 83 rad/min and a total absorbed dose of about 320 krad [18]. For a Si ring resonator, a very linear resonance wavelength shift during

Optics EXPRESS

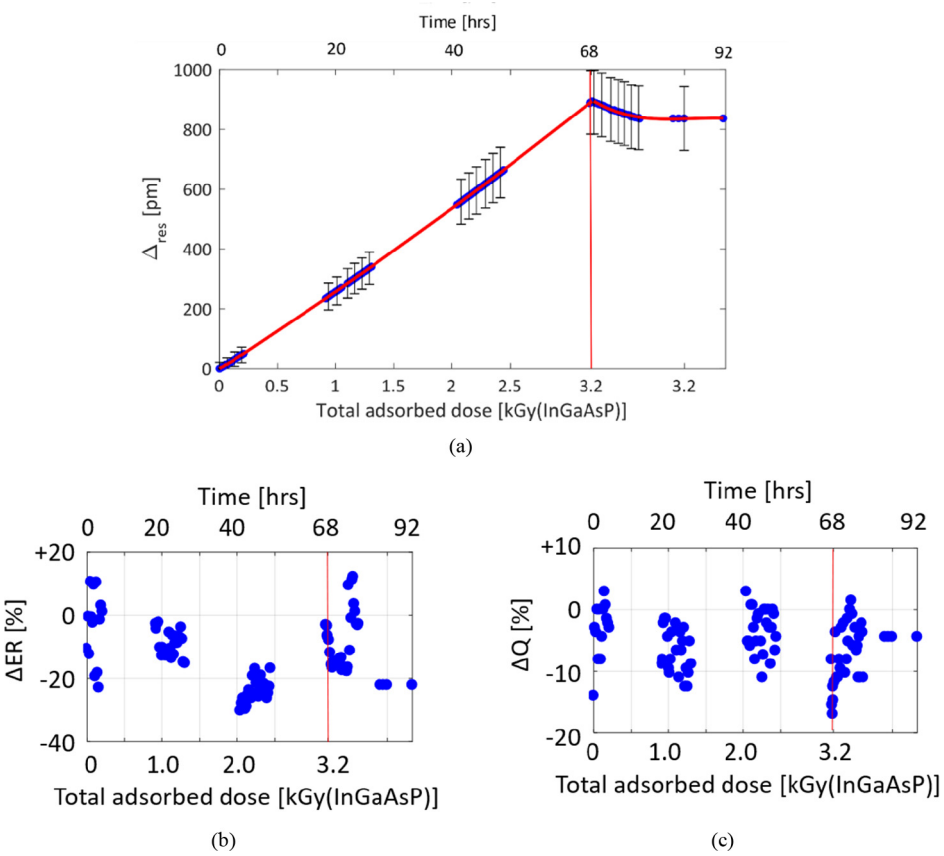

Fig. 5. (a) Red-shift of ring resonator resonance $\Delta\lambda_{res}$ vs total adsorbed dose. The bold red line is related to a linear fitting of the measured blue markers. (b) *ER* variation (ΔER) vs total adsorbed dose; (c) *Q*-factor variation (ΔQ) vs total adsorbed dose. The radiation and annealing activities are defined to the left and to the right of red line, respectively.

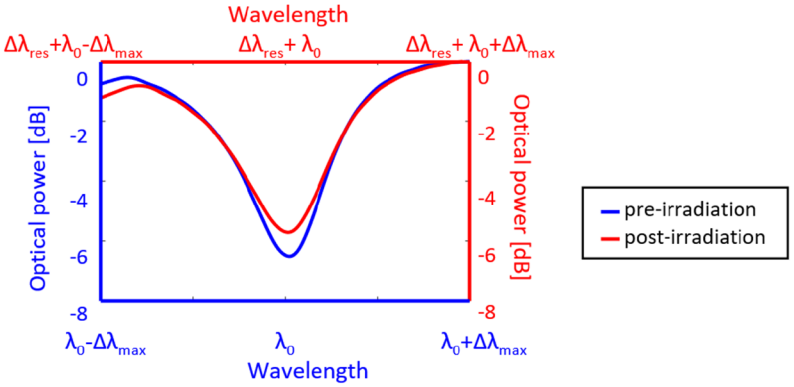

Fig. 6. TE resonance spectra pre- and after- irradiation ($\lambda_0 \approx 1.55\,\mu m$; $\Delta\lambda_{max}$ is the maximum value of the laser scan across the operating wavelength λ_0 (200 MHz); $\Delta\lambda_{res}$ is the resonance detuning, caused by the radiation effect).

Optics EXPRESS

irradiation was detected, with a slope of 0.33 pm/krad, and then with a maximum shift of about 0.1 nm at 300 krad. Furthermore, the extinction ratio of the resonance decreases of about 18% with respect to the pre-irradiation value.

Using the device under test as sensing element in an *RMOG*, the angular velocity can be calculated by the difference of the resonant frequencies, related to the clockwise and counter-clockwise waves that travel through the ring resonator, according to the Sagnac effect. Since the two waves suffer from the same resonance red-shift induced by γ radiation, the angular velocity measurement is not affected by the shift. Moreover, the slight change of Q-factor has not significant influences on the gyro resolution: a theoretical resolution of about 11 °/h has been calculated, at 320 krad with a Q mean variation of -13%. Therefore, an RMOG based on a passive InGaAsP/InP ring resonator, when used on board of a spacecraft, in addition to the advantages of using optical components, e.g. reduced weight, volume, absence of electromagnetic interference, can take advantage also of a high radiation resistance, with a consequent increase of the reliability in an environment where replacement of faulty components is best avoided.

Other space applications where the tested device can be used with very significant advantages are relevant to telecom systems and subsystems, such as filters, delay lines, beam formers, etc.

4. Conclusions

The *Co60* γ radiation impact on a high-Q InGaAsP/InP ring resonator to be used in space applications, has been estimated for the first time, to our knowledge. The fabricated device is based on an InGaAsP/InP rib waveguide, 2 µm wide and 0.3 µm thick, manufactured on a 0.7 µm thick slab layer, on an InP substrate. The resonator chip, with a footprint of about 530 mm^2, has been packaged into a brass case, including a thermoelectric controller and a thermistor. Under pre-irradiation conditions we have measured $Q = 1.36 \times 10^6$ and $ER = 6.24$ dB at about 1.55 µm for the TE mode. After irradiating the device with *Co60* γ rays with a dose of about 320 krad, we observed that slight changes were induced on both Q-factor (13%) and ER (4%). Furthermore, we have also found that the Compton scattering induced by the γ radiation, implies a refractive index change, and then a resonance red-shift, with a linear behaviour. A maximum detuning of about 800 pm has indeed been measured at about 320 krad, attenuated by a blue-offset of 60 pm during the annealing step. Our experimental study is focused only on total ionizing dose effects. Although obtained in the framework of silicon photonics, some recent results in literature [39] suggest that single event effects (SEEs) should be carefully studied to fully evaluate the radiation hardness of integrated micro-photonic devices, in other material systems, including the InP-based resonator whose behaviour under gamma irradiation has been experimentally investigated in this paper. The theoretical/experimental analysis on SEEs could be the topic of a future work. The performed results confirm the device under test as key element in several Space systems. As an example, using the device as sensitive element in a RMOG configuration, a theoretical resolution of about 9 °/h and 11 °/h has been calculated, before and after the radiation test. After irradiating it, the slight detuning of the resonance, caused by the radiation, could be assumed as common-mode noise in RMOG configuration, which means that the angular velocity measurement is not substantially affected by γ radiation. Preserving substantially its performance in Space, i.e. in a harsh environment, the ring resonator in III-V semiconductor material assumes an essential role in the design and manufacturing of the next future advanced photonic monolithically integrated devices and systems for space applications.

Funding

European Space Agency (ESA) (NPI reference: 367-2014).

Optics EXPRESS

Acknowledgments

The Authors wish to thank A. Meoli, M. Muschitiello and A. Costantino, from ESA-ESTEC, for their technical support.

References

1. J. R. Schwank, "Basic mechanisms of radiation effects in the natural space radiation environment", (No. SAND-94-1580C; CONF-940726-12). Sandia National Labs., Albuquerque, NM (United States), (1994).
2. E. R. Benton and E. V. Benton, "Space radiation dosimetry in low-Earth orbit and beyond," Nucl. Instrum. Methods Phys. Res., Sect. B **184**(1-2), 255–294 (2001).
3. IARC Working Group on the Evaluation of Carcinogenic Risks to Humans, World Health Organization, & International Agency for Research on Cancer, *Non-ionizing Radiation: Static and extremely low-frequency (ELF) electric and magnetic fields*, 80, (World Health Organization, 2002).
4. E. G. Stassinopoulos and J. P. Raymond, "The space radiation environment for electronics," Proc. IEEE **76**(11), 1423–1442 (1988).
5. O. Adriani, M. Ambriola, G. Barbarino, L. M. Barbier, S. Bartalucci, G. Bazilevskaja, R. Bellotti, S. Bertazzoni, V. Bidoli, M. Boezio, E. Bogomolov, L. Bonechi, V. Bonvicini, M. Boscherini, U. Bravar, F. Cafagna, D. Campana, P. Carlson, M. Casolino, M. Castellano, G. Castellini, E. R. Christian, F. Ciacio, M. Circella, R. D'Alessandro, C. N. De Marzo, M. P. De Pascale, N. Finetti, G. Furano, A. Gabbanini, A. M. Galper, N. Giglietto, M. Grandi, A. Grigorjeva, F. Guarino, M. Hof, S. V. Koldashov, M. G. Korotkov, J. F. Krizmanic, S. Krutkov, J. Lund, B. Marangelli, L. Marino, W. Menn, V. V. Mikhailov, N. Mirizzi, J. W. Mitchell, E. Mocchiutti, A. A. Moiseev, A. Morselli, R. Mukhametshin, J. F. Ormes, G. Osteria, J. V. Ozerov, P. Papini, M. Pearce, A. Perego, S. Piccardi, P. Picozza, M. Ricci, A. Salsano, P. Schiavon, G. Scian, M. Simon, R. Sparvoli, B. Spataro, P. Spillantini, P. Spinelli, S. A. Stephens, S. J. Stochaj, Y. Stozhkov, S. Straulino, R. E. Streitmatter, F. Taccetti, M. Tesi, A. Vacchi, E. Vannuccini, G. Vasiljev, V. Vignoli, S. A. Voronov, Y. Yurkin, G. Zampa, and N. Zampa, "The PAMELA experiment on satellite and its capability in cosmic rays measurements," Nucl. Instrum. Methods Phys. Res., Sect. A **478**(1-2), 114–118 (2002).
6. M. Boscherini, O. Adriani, M. Bongi, L. Bonechi, G. Castellini, R. D'Alessandro, A. Gabbanini, M. Grandi, W. Menn, P. Papini, S. B. Ricciarini, M. Simon, P. Splillantini, S. Straulino, F. Taccetti, M. Tesi, and W. Vannuccini, "Radiation damage of electronic components in space environment," Nucl. Instrum. Methods Phys. Res., Sect. A **514**(1-3), 112–116 (2003).
7. J. L. Barth and E. Stassinopoulos, "Space, Atmospheric, and Terrestrial Radiation Environments," IEEE Trans. Nucl. Sci. **50**(3), 466–482 (2003).
8. S. Bourdarie and M. Xapsos, "The Near-Earth Space Radiation Environment," IEEE Trans. Nucl. Sci. **55**(4), 1810–1832 (2008).
9. W. Heitler, *The quantum theory of radiation*, (Courier Corporation, 1984).
10. T. P. Ma and P. V. Dressendorfer, *Ionizing radiation effects in MOS devices and circuits*, (John Wiley & Sons, 1989).
11. F. Larin, *Radiation Effects in Semiconductor Devices*, (Wiley, 1968).
12. C. E. Barnes and J. J. Wiczer, "Radiation Effects in Optoelectronics Devices," (No. SAND-84-0771). Sandia National Labs., Albuquerque, NM (United States), (1984).
13. C. Ciminelli, F. Dell'Olio, and M. N. Armenise, *Photonics in Space: Advanced Photonic Devices and Systems*, (World Scientific, 2016).
14. H. Lischka, H. Henschel, W. Lennartz, and K. U. Schmidt, "Radiation sensitivity of light emitting diodes (LED), laser diodes (LD) and photodiodes (PD)," IEEE Trans. Nucl. Sci. **39**(3), 423–427 (1992).
15. K. A. Gill, G. Cervelli, R. Grabit, F. B. Jensen, and F. Vasey, "Radiation damage and annealing in 1310-nm InGaAsP/InP lasers for the CMS tracker," In *Photonics for Space Environments VII* (International Society for Optics and Photonics, 2000), 4134, pp. 176–185.
16. V. Brasch, Q. F. Chen, S. Schiller, and T. J. Kippenberg, "Radiation hardness of high-Q silicon nitride microresonators for space compatible integrated optics," Opt. Express **22**(25), 30786–30794 (2014).
17. S. Bhandaru, S. Hu, D. M. Fleetwood, and S. M. Weiss, "Total Ionizing Dose Effects on Silicon Ring Resonators," IEEE Trans. Nucl. Sci. **62**(1), 323–328 (2015).
18. P. Dumon, R. Kappeler, D. Barros, I. Mc Kenzie, D. Doyle, and R. Baets, "Measured radiation sensitivity of Silica-on-Silicon and Silicon-on-insulator micro-photonic devices for potential space application," In *Photonics for Space Environments X*. (International Society for Optics and Photonics, August), 5897, p. 58970D, (2005).
19. Z. Ahmed, L. T. Cumberland, N. N. Klimov, I. M. Pazos, R. E. Tosh, and R. Fitzgerald, "Assessing Radiation Hardness of Silicon Photonic Sensors," Sci. Rep. **8**(1), 13007 (2018).
20. A. H. Johnston, "Radiation Effects in Light-Emitting and Laser Diodes," IEEE Trans. Nucl. Sci. **50**(3), 689–703 (2003).
21. A. F. Fernandez, B. Brichard, and F. Berghmans, "In situ measurement of refractive index changes induced by gamma radiation in germanosilicate fibers," IEEE Photonics Technol. Lett. **15**(10), 1428–1430 (2003).
22. S. Girard, A. Morana, A. Ladaci, T. Robin, L. Mescia, J. J. Bonnefois, M. Boutillier, J. Mekki, A. Paveau, B. Cadier, E. Marin, Y. Ouerdane, and A. Boukenter, "Recent advances in radiation-hardened fiber-based technologies for Space applications," J. Opt. **20**(9), 093001 (2018).

Optics EXPRESS

23. R. S. Evenblij, T. van Leest, and M. B. Haverdings, "Integrated photonics for fiber optic based temperature sensing," In *International Conference on Space Optics—ICSO 2016* (International Society for Optics and Photonics, 2017), 10562, p. 1056210.
24. W. Primak, "Fast-Neutron-Induced Changes in Quartz and Vitreous Silica," Phys. Rev. **110**(6), 1240–1254 (1958).
25. A. H. Johnston, "Radiation effects in optoelectronic devices," IEEE Trans. Nucl. Sci. **60**(3), 2054–2073 (2013).
26. C. Ciminelli, G. Brunetti, F. Dell'Olio, F. Innone, D. Conteduca, and M. N. Armenise, "Emerging Applications of Whispering Gallery Mode Photonic Resonators," In *International Conference on Applications in Electronics Pervading Industry, Environment and Society* (Springer, Cham., 2016), pp. 185–191.
27. F. Dell'Olio, T. Tatoli, C. Ciminelli, and M. N. Armenise, "Recent advances in miniaturized optical gyroscopes," J. of the Eur. Opt. Soc.-Rap. Publ. **9**, 14013 (2014).
28. F. Dell'Olio, C. Ciminelli, M. N. Armenise, F. M. Soares, and W. Rehbein, "Design, fabrication, and preliminary test results of a new InGaAsP/InP high-Q ring resonator for gyro applications," In *2012 International Conference on Indium Phosphide and Related Materials (IPRM)*, (IEEE, 2012), pp. 124–127.
29. C. Ciminelli and M. N. Armenise, "Final report", ESA-founded project MiOS (Micro Optical Angular Velocity Sensor), November, 2014.
30. C. Ciminelli, F. Dell'Olio, M. N. Armenise, F. M. Soares, and W. Passenberg, "High performance InP ring resonator for new generation monolithically integrated optical gyroscopes," Opt. Express **21**(1), 556–564 (2013).
31. U. Fano, "Effects of configuration interaction on intensities and phase shifts," Phys. Rev. **124**(6), 1866–1878 (1961).
32. S. Ezekiel and S. R. Balsamo, "Passive ring resonator laser gyroscope," Appl. Phys. Lett. **30**(9), 478–480 (1977).
33. W. Bogaerts, P. De Heyn, T. Van Vaerenbergh, K. De Vos, S. K. Selvaraja, T. Claes, P. Dumon, P. Bienstman, D. Van Thourhout, and R. Baets, "Silicon microring resonators," Laser Photonics Rev. **6**(1), 47–73 (2012).
34. A. Yariv, "Critical coupling and its control in optical waveguide-ring resonator systems," IEEE Photonics Technol. Lett. **14**(4), 483–485 (2002).
35. A. Waqas, A. Alippi, D. Melati, and A. Melloni, "An improved model to predict thermo-optic coefficient in InGaAsP waveguides," In *2016 18th International Conference on Transparent Optical Networks (ICTON)*, (IEEE, 2016), (pp. 1–4)
36. Total Dose Steady-State Irradiation Test Method, ECSS European Space Components Coordination, 5, June 2016. http://escies.org/escc-specs/published/22900.pdf.
37. Co-60 source at ESA-ESTEC. https://escies.org/webdocument/showArticle?id=251.
38. R. L. Pease, G. W. Dunham, J. E. Seiler, D. G. Platteter, and S. S. McClure, "Total dose and dose rate response of an AD590 temperature transducer," IEEE Trans. Nucl. Sci. **54**(4), 1049–1054 (2007).
39. P. S. Goley, Z. E. Fleetwood, and J. D. Cressler, "Potential Limitations on Integrated Silicon Photonic Waveguides Operating in a Heavy Ion Environment," IEEE Trans. Nucl. Sci. **65**(1), 141–148 (2018).